Indian Journal of Chemistry
Vol. 58A, April 2019, pp. 429-435

Exploring the mechanism of conversion of monosulfiram into disulfiram

Vineet Kumar Singh, Sukirti Gupta & Ashutosh Gupta*
Department of Chemistry, Udai Pratap Autonomous College, Varanasi 221 002, India
Email: ashu1809@gmail.com

Received 30 August 2018; revised and accepted 18 February 2019

Monosulfiram is a drug used topically in the treatment of scabies. Upon its application it shows similar effects as seen in case of disulfiram, a drug used in alcohol aversion therapy. Previous reports have concluded a light induced conversion of monosulfiram (MS) into disulfiram (DS). In the present study a computational approach has been involved to investigate the mechanism of this conversion. Structures have been optimized using MP2 and DFT approach. Insights on their reactivities have been assessed through conceptual DFT. Time-dependent DFT investigation has been undertaken to obtain excitation energies for singlet and triplet states. Bond dissociation energies of both molecules have also been obtained and analyzed. It has been found that conversion of MS into DS occurs in both thermal and photochemical situations.

Keywords: Monosulfiram, Disulfiram, *Ab initio*, Density functional theory, Bond dissociation energy, Natural population analysis, Conceptual density functional theory, Potential energy surface, Time dependent-density functional theory

Monosulfiram (tetraethylthiuram monosulfide) (MS) (Fig. 1a) is one among the chemical constituents, which are extensively utilized in the treatment of scabies. However, medical complications such as vomiting, nausea, tachycardia and flushing are reported in some individuals[1-4]. These side effects are also observed in those patients, who are administered disulfiram (tetraethylthiuram disulfide) (DS) (Fig. 1b), a drug, used in the treatment of alcohol aversion therapy. Alcohol dehydrogenase catalyzes ethanol to acetaldehyde which is then oxidized to acetic acid by aldehyde dehydrogenase (ALDH2). Inhibition of ALDH2 by DS *in vivo* leads to accumulation of acetaldehyde which causes aversive conditions[5-7]. It is reported that disulfide linkage formation takes place between sulfur atoms of DS and ALDH, thus impairing the activity of ALDH[8-9].

It has been proposed that MS gets converted into DS in the presence of light during or prior to its topical application[10]. There are evidences that generation of free radicals is involved during the formation of DS from MS, as is evident from the reports on generation of free radical species during the photolysis of organic disulfide compounds[11]. Tetramethylthiuram monosulfides (TMS) and tetramethylthiuram disulfides (TMD), analogues of MS and DS, respectively, are found to initiate free radical polymerization via thermal and photochemical pathways[12-14]. Considerably high amount of homolytic cleavage of C-S bond is found to occur in visible light for TMS[13].

The present study deals with the computational investigation of the mechanism of conversion of monosulfiram into disulfiram. The study is important not only from the point of view of extensive application of sulfur containing compounds in polymer and medicinal industry but also because of their role in environmental chemistry. Various thiuram disulfides such as TMS (thiram) are used as agricultural fungicides and pesticides, and, extensive

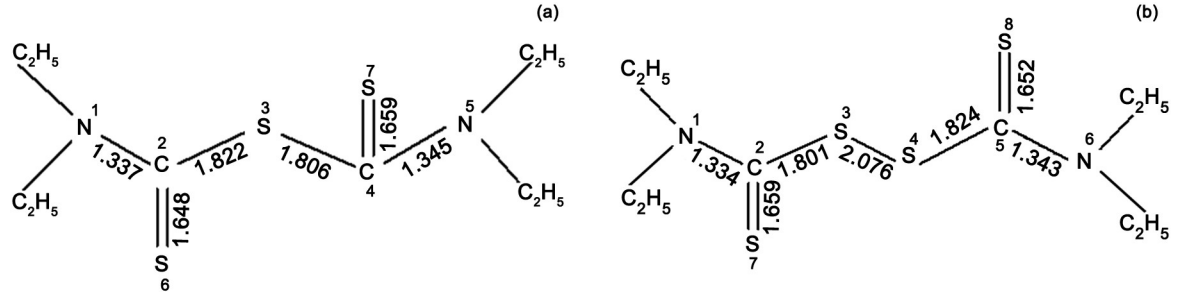

Fig. 1 — (a) Structure and bond lengths of monosulfiram at M06-2X/6-311++G(d,p) level, and, (b) structure and bond lengths of disulfiram at M06-2X/6-311++G(d,p) level.

photochemical studies are carried out on such compounds[15-17]. Overdose of disulfiram is reported to cause psychotic disorders in some patients[18]. It is anticipated that topical application of MS can also cause such symptoms. Therefore it becomes even more important to understand underlying mechanism of MS to DS conversion.

In order to elucidate the reaction mechanism of conversion of MS into DS, structures and energetics of MS and DS are computed at the MP2 and DFT levels of theory. Their reactivities and properties are assessed by employing conceptual density functional theory (CDFT). Excited state potential energy surface has been obtained using time dependent density functional theory (TDDFT).

Materials and Methods

Computational details

All density functional theory (DFT) and *ab initio* calculations are carried out using Gaussian 09 suite of programs[19]. Geometries are optimized in gaseous phase with the B3LYP[20], M06-2X hybrid functional[21] and MP2 level of theory[22] in conjunction with different Pople basis sets[23]. Vertical excitation energies are calculated with time-dependent DFT[24] methodology using the DFT functionals such as B3LYP, BH&HLYP, BLYP and M06-2X and different Pople basis sets. Natural bond order (NBO) charge distribution and bond dissociation energies of target molecules are computed. The nature of the stationary point is characterized by harmonic frequency calculations. Bond dissociation energy is computed for the targeted molecules with different DFT functionals and basis sets as follows:

$$\text{BDE (A-B)} = \text{E(A-B)} - \text{E(A}\bullet\text{)} - \text{E(B}^{\cdot}\text{)} \quad ...(1)$$

where E denotes total energy.

Different conceptual DFT based reactivity descriptors are utilized to assess different properties of target molecules.

For an N-electron system, the electronegativity[25,26] (χ) and hardness[27] (η) can be defined as follows:

$$\chi = -\mu = -\left(\frac{\partial E}{\partial N}\right)_{v(\vec{r})} \quad ...(2)$$

$$\eta = \left(\frac{\partial \mu}{\partial N}\right)_{v(\mathbf{r})} = \left(\frac{\partial^2 E}{\partial N^2}\right)_{v(\mathbf{r})} \quad ...(3)$$

where E is the total energy of the N-electron system and μ and $v(\vec{r})$ are its chemical potential and external potential, respectively. The electrophilicity[28] (ω) is defined as

$$\omega = \frac{\mu^2}{2\eta} = \frac{\chi^2}{2\eta} \quad ...(4)$$

A finite difference approximation to eqns 2 and 3 can be expressed as

$$\chi = \frac{I + A}{2} = -\mu \quad ...(5)$$

and $\eta = I - A$ ...(6)

where I and A are the ionization potential and electron affinity of the system, respectively. I and A are computed using Koopmans' theorem[26]. It may be worthy mentioning that Koopmans' theorem is strictly valid within the Hartree-Fock theory. However, one may use this in Kohn-Sham computations with the help of Janaks' theorem[29].

The local reactivity descriptor, Fukui function[30] ($f(\vec{r})$) represents the change in electron density at a given point when an electron is added to or removed from a system at constant $v(\vec{r})$. It can be representated as:

$$f(\mathbf{r}) = \left(\frac{\partial \rho(\mathrm{r})}{\partial N}\right)_{v(\mathbf{r})} = \left(\frac{\delta \mu}{\delta v(\mathbf{r})}\right)_N \quad ...(7)$$

Condensation of this Fukui function, $f(\vec{r})$ to an individual atomic site k in a molecule gives rise to the following expressions in terms of electron population[31,32] q_k

$$f^+(\mathbf{r}) = \left(\frac{\partial \rho(\mathbf{r})}{\partial N}\right)^+_{v(\mathbf{r})} \approx \rho_{\mathrm{N+1}}(\mathbf{r}) - \rho_{\mathrm{N}}(\mathbf{r}) \approx \rho_{\mathrm{LUMO}}(\mathbf{r})$$

for nucleophilic attack ...(8a)

$$f^-(\mathbf{r}) = \left(\frac{\partial \rho(\mathrm{r})}{\partial N}\right)^-_{v(\mathbf{r})} \approx \rho_{\mathrm{N}}(\mathbf{r}) - \rho_{\mathrm{N-1}}(\mathbf{r}) \approx \rho_{\mathrm{HOMO}}(\mathbf{r})$$

for electrophilic attack ...(8b)

$$f^0(\mathbf{r}) = \frac{1}{2}\left[f^+(\mathbf{r}) + f^-(\mathbf{r})\right] \text{ for radical attack} \quad ...(8c)$$

Chattaraj *et al.,* have proposed a generalized concept of philicity at a given atomic site k[33]. The condensed-to-atom variants of it for the atomic site k have been written as

$$\omega_k^{\alpha} = \omega f_k^{\alpha} \quad ...(9)$$

where α = +, −, and 0 refer to nucleophilic, electrophilic, and radical attacks, respectively.

The condensed philicity summed over a group of relevant atoms is termed as the 'group philicity' [34] and can be expressed as

$$\omega_g^\alpha = \sum_{k=1}^{n} \omega_k^\alpha \quad \ldots(10)$$

where n is the number of atoms coordinated to the reactive atom, ω_k^α and ω_g^α are the local philicity of the atom, and the group philicity, respectively.

The net electrophilicity ($\Delta\omega^\pm$), a new dual descriptor proposed recently by Chattaraj *et al*., is a measure of the electron accepting power relative to the electron donating power of a given species[35].

The mathematical genesis of net electrophilicity ($\Delta\omega^\pm$) stems from an earlier idea of the concept of the electron accepting (ω^+) and electron donating (ω^-) powers enunciated by Gazquez and co-workers[36]. Gazquez *et al*., have defined the latter quantities as follows:

$$\omega^+ = \frac{EA^2}{2(IP - EA)} \quad \ldots(11)$$

$$\omega^- = \frac{IP^2}{2(IP - EA)} \quad \ldots(12)$$

$$\Delta\omega^\pm = \left\{\omega^+ - \left(-\omega^-\right)\right\} = \left(\omega^+ + \omega^-\right) \quad \ldots(13)$$

Results and Discussion

Geometry

Different geometrical parameters of MS and DS have been optimized at the B3LYP, M06-2X and MP2-FC (frozen core) levels of theory with different basis sets (Supplementary Data, Tables S1-S2). The parameters obtained from the MP2 computation are considered as reference, and accordingly it is found that M06-2X/6-311++G(d,p) gives the best result among all the methods. The different bond parameter values reported in Fig. 1 correspond to M06-2X/6-311++G(d,p) level of theory. Both MS and DS are found to be slightly unsymmetrical. Such an unsymmetry is also elucidated through XRD studies of Disulfiram molecule and can be attributed to extended conjugation present in both MS and DS[37]. Dihedral angle in MS for C(=S)SC(=S)N is −172.8° denoting the atoms under consideration as almost planar. Similarly, SSCS(C=S) dihedral angle is 0.4°, reflecting those atoms to be placed on a plane. The structural parameters clearly reflect that in case of MS, the two C-S bonds being the longest bonds (1.806 Å, 1.822 Å) are more vulnerable to bond dissociation. Similarly, the S-S bond in DS with a bond length of 2.076 Å, which is longer than usual, is most likely to get dissociated on absorption of appropriate energy.

Ground state studies

Bond dissociation energy

Bond dissociation energy (BDE) of C-S and S-S bonds in case of MS and DS respectively, computed with different DFT functionals and basis sets are shown in Table 1. BDE of MS varies from 32.5 to 49.0 kcal mol^{-1} at different levels. Similarly, DS has BDE in the range of 12.2 to 29.1 kcal mol^{-1}. The energy difference (ΔE) between BDE values for MS and DS remains more or less the same for all basis sets and functionals except B3LYP/6-311G(d,p) which seems to overestimate the BDE of MS and underestimate the BDE of DS. Considering the fact that the best structural parameters in the present study is found at the M06-2X/6-311++G(d,p) level in comparison to MP2-FC/6-311++G(d,p), we presume MS possesses BDE of 48.9 kcal mol^{-1}, whereas, DS has BDE of 29.1 kcal mol^{-1}. Therefore, for the conversion of MS into DS under thermal conditions, energy close to 48.9 kcal mol^{-1} is required for the generation of free radicals, which could re-unite to form DS.

Reactivity

Conceptual density functional theory (CDFT) has evolved as a versatile tool to discuss different properties of a molecule. Different descriptors such as electronegativity (χ), chemical potential (μ), electrophilicity (ω), net electrophilicity ($\Delta\omega$), etc., are determined for MS and DS at the B3LYP/6-311++G(d,p) level, and the values are shown in Table 2. Net electrophilicity values of MS and DS found as 7.4 eV, and 7.6 eV, respectively, also reflect good reactivity properties of these

Table 1 — Bond dissociation energy of (kcal mol^{-1}) monosulfiram and disulfiram at different levels of theory

	monosulfiram (C-S)	disulfiram (S-S)	ΔE
B3LYP/6-31+G(d,p)	33.4	14.3	19.1
B3LYP/6-311G(d,p)	43.2	12.2	31.0
B3LYP/6-311++G(d,p)	32.5	13.7	18.8
M06-2X/6-31+G(d)	49.0	29.1	19.9
M06-2X/6-311G(d,p)	33.9	16.4	17.5
M06-2X/6-311++G(d,p)	48.9	29.1	19.8

molecules. Among MS and DS, DS shows more reactivity on account of its high net electrophilicity. However, the chemical properties of both MS and DS are comparable, and, therefore, it is expected that both show similar properties. In order to assess the site selectivity in MS and DS molecules, local philicities are computed at the B3LYP/6-311++G(d,p) level, and are shown in Tables 3(a) and 3(b), respectively. The atomic charge based on Mulliken population analysis (MPA) and natural population analysis (NPA) are also provided. Fukui functions and different types of electrophilicities on individual atoms of MS and DS are calculated based on MPA charge. Based on NPA values, both the nitrogen atoms (1N, 5N) of MS are found to have negative charge of −0.48 e^- and −0.50 e^-, respectively. On the other hand, both carbon atoms (2C, 4C) are only slightly negatively charged with values of −0.07 e^- and −0.08 e^-, respectively. Similarly, both sulfur atoms doubly bonded to carbon atoms (6S, 7S) also possess slightly negative charge (−0.08 e^-, −0.15 e^-). However, the sulfur atom (3S) acting as a bridge to two –NC(=S) units is found to be positively charged (0.26 e^-) indicating the deficiency of electron on it. This reflects conjugation phenomenon undergoing within MS molecule leading to electron accumulation at sulfur atoms doubly bonded to carbon atoms at the cost of electron loss from bridging sulfur (3S) atom. The same trend is observed for DS wherein NPA charges for 1N, 2C, 5C, 6N, 7S and 8S are found to be more negative with respect to two bridging sulfur atoms (0.21 e^- and 0.08 e^-) indicating the transfer of electrons from them to other connecting atoms through conjugation. Further, positive charges on these two sulfur atoms make them more vulnerable for homolytic fission leading to the formation of free radicals. This substantiates its utility in polymer chemistry. The above discussion clearly justifies the reason for the formation of free radicals in thermal conditions in case of MS and DS. Thus, MS can form DS in the presence of heat, although the stability of DS in the same environment is not guaranteed.

Excited state studies

In order to understand the photolytic conversion of MS into DS, it is required that the photo-physical

Table 2 — Global descriptors of monosulfiram and disulfiram

Molecules	χ(eV)	μ (eV)	η(eV)	ω (eV)	ω^+	ω^-	$\Delta\omega^\pm$
Monosulfiram	3.70	-3.70	3.67	1.86	0.0001	7.41	7.40
Disulfiram	3.82	-3.82	3.64	2.01	0.01	7.66	7.66

Table 3 — Local descriptors of (a) monosulfiram and (b) disulfiram based on conceptual DFT parameters

Atom	MPA (au) Neutral	NPA (au) Neutral	MPA (au) Cation	MPA (au) Anion	f_k^+ (au)	f_k^- (au)	ω_k^+	ω_k^-
			(a) Monosulfiram					
1N	0.52	-0.48	0.51	0.51	-0.00	0.01	-0.01	0.01
2C	-0.06	-0.07	0.01	0.10	0.17	-0.07	0.31	-0.12
3S	0.30	0.26	0.42	0.15	-0.15	-0.12	-0.27	-0.23
4C	-0.68	-0.08	-0.68	-0.65	0.03	-0.01	0.06	-0.01
5N	0.54	-0.50	0.53	0.54	-0.00	0.01	-0.01	0.03
6S	-0.50	-0.08	-0.21	-0.78	-0.28	-0.29	-0.52	-0.54
7S	-0.53	-0.15	-0.34	-0.60	-0.08	-0.19	-0.14	-0.35
Whole molecule	0.001	0.001	0.998	-0.997	-0.998	-0.997	-1.862	-1.860
			(b) Disulfiram					
1N	0.46	-0.49	0.45	0.43	-0.02	0.01	-0.04	0.02
2C	0.32	-0.07	0.20	0.41	0.09	0.13	0.18	0.26
3S	-0.41	0.21	-0.18	-0.53	-0.12	-0.22	-0.25	-0.44
4S	0.56	0.08	0.53	0.58	0.02	0.02	0.04	0.05
5C	-0.71	-0.08	-0.54	-0.79	-0.08	-0.17	-0.15	-0.35
6N	0.55	-0.50	0.51	0.56	0.01	0.03	0.03	0.07
7S	-0.58	-0.11	-0.33	-0.82	-0.23	-0.25	-0.47	-0.51
8S	-0.49	-0.12	-0.31	-0.65	-0.15	-0.18	-0.31	-0.37
Whole molecule	-0.001	0.001	1 .000	-1.003	-1.002	-1.001	-2.016	-2.014

NPA = Natural Population Analysis; MPA = Mulliken Population Analysis

properties of MS and DS be investigated. Vertical excitation energies of MS and DS (singlet and triplet excitation energies up to first three levels) for gaseous phase are computed by using different DFT functionals, and are shown in Tables 4(a) and 4(b). Various DFT functionals such as B3LYP, BH&HLYP, BLYP and M06-2X are employed for the determination of excitation energies. The first singlet excitation energy ranges from 2.8 eV (65.0 kcal mol^{-1}) to 3.4 eV (79.4 kcal mol^{-1}) for MS. The second singlet excitation energy ranges from 2.8 eV to 3.9 eV. The third singlet excitation energy for MS is in the range of 3.1 eV to 4.1 eV. As the visible light ranges from 1.6 eV to 3.4 eV, it is expected that MS can get excited to first, second and above singlet excited energy levels in presence of visible light. First singlet excitation energies of DS ranges from 2.9 eV to 3.7 eV, whereas, the second singlet excitation energy varies from 3.01 eV to 3.8 eV, and for third singlet excitation energy is in the interval of 3.1 eV to 3.9 eV. Thus, DS requires more energy in comparison to MS to reach its first singlet excited state. Though DS can get excited by visible light to its first and other singlet excited states, it would be worth noting that the excitation energy for DS is on an average, larger than that of MS which implies its greater stability than MS in the presence of light. This observation is contrary to what is seen in case of thermal dissociation of DS wherein it undergoes thermal dissociation more easily in comparison to MS. Thus, MS in presence of light gets easily excited in comparison to DS making it more vulnerable to photolytic dissociation.

Table 4 — Excitation energy values (from S_0) of (a) monosulfiram and (b) disulfiram

	Excitation Energies (eV)			
	(a) Monosulfiram			
	B3LYP/ 6-31+G(d)	BH&HLYP/ 6-31+G(d)	BLYP/ 6-31+G(d)	M06-2X/ 6-31+G(d)
T_1	2.6	2.4	2.6	2.7
T_2	2.7	2.9	2.7	3.0
T_3	3.2	3.1	2.8	3.3
S_1	2.9	3.2	2.8	3.2
S_2	3.4	3.6	2.8	3.6
S_3	3.4	3.9	3.1	3.8
	(b) Disulfiram			
T_1	2.9	2.9	2.7	3.0
T_2	3.1	3.1	2.9	3.2
T_3	3.2	3.3	3.1	3.2
S_1	3.3	3.5	3.0	3.3
S_2	3.3	3.6	3.0	3.4
S_3	3.5	3.8	3.1	3.5

T_1: First triplet state S_1: First singlet state
T_2: Second triplet state S_2: Second singlet State
T_3: Third triplet state S_3: Third singlet state

In order to have a deeper insight into the mechanism of conversion of MS into DS, potential energy surfaces of MS and DS both in ground and excited states are generated by relaxed scan at the M06-2X/6-31+G(d) level, and are shown in Fig. 2(a) and (b), respectively. Figure 2(a) depicts the thermal and photochemical dissociative pathway of MS. C-S bond length is considered as reaction profile as it is more prone towards dissociation. A 'shoulder' is observed at 2.7 Å C-S bond length. To reach this point, MS molecule at S_0 potential energy surface (PES) needs to cross a barrier of around 1.7 eV. The whole molecule gets dissociated into free radicals at around 3.1 eV. However, to excite MS to S_1 energy level, 3.0 eV of energy is required. This further requires around 1.0 eV more energy to cross the S_1 barrier and follow the photochemical reaction pathway. Overall, around 4 eV of energy is required for the photochemical dissociation of MS. This excited energy level is closer to 'near' visible range, and, therefore, is accessible by the molecule in presence of sunlight. Since S_1 and T_1 are closer in energy, hence, there exists a possibility wherein energy from S_1 energy state gets transferred to T_1 energy state through inter-system crossing (ISC) phenomenon. The energy gap between S_1 and T_1 reduces significantly around 2.6 Å. Thus, on absorption of light, MS can get excited to S_1 energy level, and then later, may get transferred to T_1 through the phenomenon of ISC to form free radicals. Such a phenomenon is reported for thiocarbonyl choromophores[21,22]. All the excited state pathways seem to converge near 4.5 Å, which could imply the spin crossing over to generate DS and other product molecules. There remains one more possibility for the conversion of MS into DS. On account of energy barrier observed in S_1 PES, MS can reach S_0 via T_1 through ISC, and, while moving along the reaction coordinate it forms free radicals which later combine to form DS. Overall, MS can get dissociated into free radicals along C-S bond both by thermolysis and photolysis. The observed energy barrier is more in S_0 PES than along S_1 PES. Thus, conversion of MS into DS is more feasible in photolytic medium. Figure 2(b) highlights the reaction energy profile of DS in thermal and photolytic environment with consideration of S-S

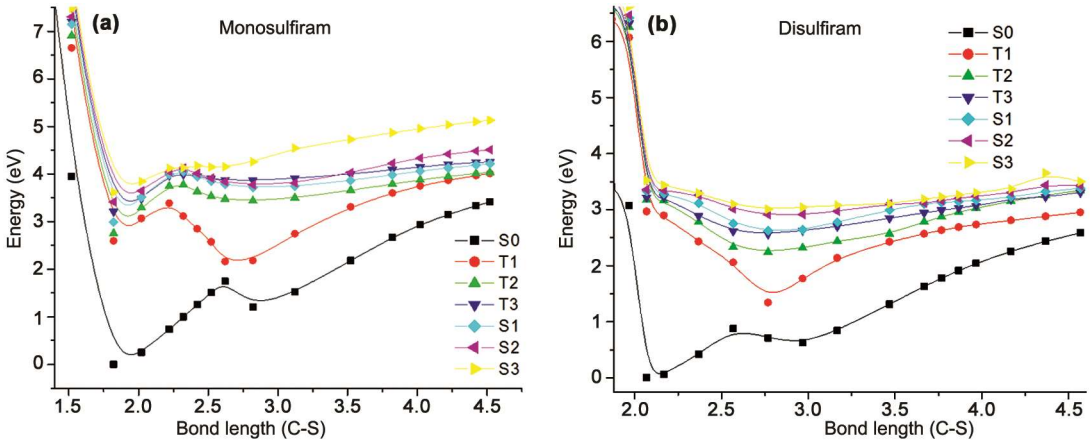

Fig. 2 — (a) Potential energy profile of monosulfiram generated at the M06-2X/6-31+G(d) level, and, (b) potential energy profile of disulfiram generated at the M06-2X/6-31+G(d) level.

bond as reaction coordinate. It is observed that very less energy in comparison to MS (0.8 eV) is required for the thermal dissociation of DS. The energy gap between S_0 and S_1 is in the range of 3.3 eV, which lies in the 'near' visible range. This is higher in comparison to that observed for MS. Considering the fact that MS dissociates into free radicals, among which, one of the possibilities of the product formation after recombination of radicals is the formation of DS, it is pertinent to look into potential energy profile of DS along S-S bond length. It can be clearly inferred from Fig. 2(b) that free radicals with symmetrical Et_2NCS moiety, tend to recombine together when these entities start coming closer to each other to form MS in both thermal and photochemical environment. Recombination of the symmetrical free radical is quite easier in case of thermal reaction ((S_0) energy state). However, in case of higher singlet energy state (S_1) its crossing occurs with third triplet energy state (T_3) on account of ISC. This further triggers IC leading to the decay of DS molecule to T_1 state. It then decays to S_0 energy state through phosphorescence phenomenon leading to the formation of stable disulfiram molecule. It is also possible that excited DS S_1 state reaches to S_0 PES through IC, which then either recombines to DS or gets thermally dissociated into radical fragments.

Conclusions

An effort has been made to gain insights into the mechanism of conversion of MS into DS in thermal and photochemical environments. Ground and excited state studies of MS and DS are carried out to know the mechanistic detail. *Ab initio* and DFT methods are employed to gather descriptive information. It is found that cleavage of MS into free radicals is possible both in thermal and photolytic conditions. Dissociation of MS in photolytic fashion is more feasible due to lesser activation barrier energy for S_1 PES than the barrier observed for S_0 PES for thermal dissociation.

Supplementary Data

Supplementary data associated with this article are available in the electronic form at http://www.niscair.res.in/jinfo/ijca/IJCA_58A(04)429-435_SupplData.pdf

Acknowledgement

AG thanks University Grants Commission, New Delhi for a major research project and VKS is thankful to CSIR, New Delhi, India for a Junior Research Fellowship. Authors also thank Dr V B Singh, Dr B K Mishra and Dr S Pan for useful discussions.

References

1 Mays D C, Nelson A N, Benson L M, Johnson K L, Naylor S & Lipsky J J, *Biochem Pharmacol*, 48 (1994) 1917.
2 Blanc D & Deprez P, *The Lancet*, 335 (1990) 1291.
3 Gold S, *The Lancet*, 288 (1966) 1417.
4 Plouvier B, Lemoine X, De Coninck P, Baclet J L & François M, *Nouv Presse Med*, 11 (1982) 3209.
5 Hald J, Jacobsen E & Larsen V, *Acta Pharmacol Toxicol*, 4 (1948) 285.
6 Graham W D, *J Pharm Pharmacol*, 3 (1951) 160.
7 Koppaka V, Thompson D C, Chen Y, Ellermann M, Nicolaou K C, Juvonen R O, Petersen D, Deitrich R A, Hurley T D & Vasiliou V, *Pharmacol Rev*, 64 (2012) 520.
8 Vallari R C & Pietruszko R, *Science*, 216 (1982) 637.
9 Deitrich R A & Erwin V G, *Mol Pharmacol*, 7 (1971) 301.
10 Lipsky J, Mays D C & Naylor S, *The Lancet*, 343 (1994) 304.
11 Lyons W, *Nature*, 162(1948) 1004.

12 Ferington T & Tobolsky A V, *J Am Chem Soc*, 77 (1955) 4510.
13 Ferington T & Tobolsky A V, *J Am Chem Soc*, 80 (1958) 3215.
14 Kern R, *J Am Chem Soc*, 77 (1955) 1382.
15 Crank G & Mursyidi A, *J Photochem Photobiol A Chem*, 68 (1992) 289.
16 Burrows H, Canle L M, Santaballa J & Steenken S, *J Photochem Photobiol B*, 67 (2002) 71.
17 Filipe O M S, Santos S A O, Domingues M R M, Vidal M M, Silvestre A J D, Neto C P & Santos E B H, *Chemosphere*, 91 (2013) 993.
18 Mohapatra S & Rath N R, *Clin Psychopharmacol Neurosci*, 15 (2017) 68.
19 Frisch M J, Trucks G W, Schlegel H B, Scuseria G E, Robb M A, Cheeseman J R, Montgomery J, Vreven T, Kudin K N & Burant J C, Gaussian 09; Gaussian, Inc: Pittsburgh, PA, (2009).
20 Becke A D, *J Chem Phys*, 98 (1993) 5648.
21 ZhaoY & Truhlar D G, *Theor Chem Acc*, 120 (2008) 215.
22 Head-Gordon M, Pople J A & Frisch M J, *Chem Phys Lett*, 153 (1988) 503.
23 Ditchfield R, Hehre W J & Pople J A, *J Chem Phys*, 54 (1971) 724.
24 Bauernschmitt R & Ahlrichs R, *Chem Phys Lett*, 256 (1996) 454.
25 Parr R G, Donnelly R A, Levy M & Palke W E, *J Chem Phys*, 68 (1978) 3801.
26 Koopmans T, *Physica*, 1 (1934) 104.
27 Parr R G & Pearson R G, *J Am Chem Soc*, 105 (1983) 7512.
28 Parr R G, Szentpály L V & Liu S, *J Am Chem Soc*, 121 (1999) 1922.
29 Janak J, *Phys Rev B*, 18 (1978) 7165.
30 Yang W, Parr R G & Pucci R, *J Chem Phys*, 81 (1984) 2862.
31 Yang W & Mortier W J, *J Am Chem Soc*, 108 (1986) 5708.
32 Lee C, Yang W & Parr R G, *Phys Rev B*, 37 (1988) 785.
33 Chattaraj P K, Maiti B & Sarkar U, *J Phys Chem A*, 107 (2003) 4973.
34 Parthasarathi R, Subramanian V, Roy D R & Chattaraj P K, *Bioorg Med Chem*, 12 (2004) 5533.
35 Chattaraj P K, Chakraborty A & Giri S, *J Phys Chem A*, 113 (2009) 10068.
36 Gazquez J L, Cedillo A & Vela A, *J Phys Chem A*, 111 (2007) 1966.
37 Karle I L, Estlin J A & Britts K, *Acta Cryst*, 22 (1967) 273.